# Proximity and Josephson effects in superconductor/antiferromagnetic Nb/$\gamma$-$Fe_{50}Mn_{50}$ heterostructures

C. Bell, E. J. Tarte, G. Burnell, C. W. Leung, D.-J. Kang, and M. G. Blamire
*Materials Science Department, IRC in Superconductivity and IRC in Nanotechnology, University of Cambridge, Cambridge, United Kingdom*

(Received 13 May 2003; revised manuscript received 26 June 2003; published 23 October 2003)

We study the proximity effect in superconductor ($S$), antiferromagnetic (AF) bilayers, and report the fabrication and measurement of the first trilayer $S$/AF/$S$ Josephson junctions. The disordered fcc alloy $\gamma$-$Fe_{50}Mn_{50}$ was used as the AF, and the $S$ is Nb. Micron and submicron scale junctions were measured, and the scaling of $J_C(d_{AF})$ gives a coherence length in the AF of 2.4 nm, which correlates with the coherence length due to suppression of $T_C$ in the bilayer samples. The diffusion constant for FeMn was found to be 1.7 $\times 10^{-4}$ $m^2\,s^{-1}$, and the density of states at the Fermi level was also obtained. An exchange biased FeMn/Co bilayer confirms the AF nature of the FeMn in this thickness regime.

DOI: 10.1103/PhysRevB.68.144517 PACS number(s): 74.45.+c, 75.50.Ee, 85.25.Cp, 85.70.Kh

## I. INTRODUCTION

From the earliest work of Hauser *et al.*[1] there has been considerable interest in the proximity effect between thin film superconductors ($S$) with both ferromagnetic ($F$) and antiferromagnetic (AF) materials. More recently Nb/Cr multilayers[2] and Nb/CuMn (spin-glass) systems have been studied,[3] as have Cr/V/Cr trilayers.[4] The recently renewed interest in the $S/F$ proximity effect due to the oscillating order parameter in the $F$ layer and the so-called $\pi$ shift, recently found experimentally,[5,6] has not led to complimentary experiments in $S$/AF heterostructures. As has been pointed out by Krivoruchko,[7] the nesting features of Fermi surfaces of the so-called band antiferromagnets destroys the symmetry in momentum space, similar to the splitting of the Fermi surface in the $F$ case. Therefore a band AF heavily suppresses superconductivity, but without the oscillating order parameter found in the $F$ case which is necessary to realize $\pi$ junctions.

There has been much theoretical literature concerning $S/F$ heterostructures (bilayer, trilayers, and multilayers: for a review see Ref. 8). The various effects on the superconducting critical temperature, field, and current density ($T_C$, $H_C$, and $J_C$) of the parallel and antiparallel configurations of the $F$ layers is of great interest. Various theoretical predictions have been made for $J_C$ enhancement in the case of $S/F/X/F/S$ Josephson junctions, when the $F$ layers have their moments switched from parallel to antiparallel, with large effects for $X$=insulator ($I$),[9–11] more weakly in the case of $X$=normal (dirty) metal ($N$).[12] Spin torque on the $F$ layers due to the Josephson current has been predicted for $X=N$.[13] To achieve these "spin-active" junctions, techniques can be borrowed from the magnetics community in the fabrication of spin-valve devices. In these cases the antiparallel alignment is achieved either by the use of two materials with different coercive fields, or by using an AF to "pin" (exchange bias) one of two otherwise identical $F$ layers. In the latter case this can be done by field cooling through the blocking temperature (which is $\leqslant T_N$, the Néel temperature), which increases the coercive field, and shifts the center of the magnetic hysteresis loop to a nonzero applied field. The latter technique was used in the $F/S/F$ trilayers studied in Ref. 14. If this technique is to be applied to the case of $S/F/X/F/S$ Josephson junctions, it is crucial to understand the Josephson effect through an AF, as the device is built up layer by layer.

The effect of magnetic and nonmagnetic impurities in the barriers of $S/N/S$ junctions has been previously studied—including the spin glasses CuMn, AgMn,[15,16] and CuNi.[17] In these cases the barrier thicknesses were of the order of 100 nm or thicker (since the impurity concentrations were relatively small: for example a maximum of 4.6 at. % Mn in the case of CuMn in Ref. 16). To our knowledge no measurements have ever been made of AF Josephson junctions and, in particular, with the AF $\gamma$-$Fe_{50}Mn_{50}$. In this paper we present bilayer $T_C$ measurements of the proximity effect between FeMn and Nb, and the first measurement of the Josephson effect through an AF. These measurements enable the coherence length in the AF to be found, and hence the diffusion constant, and in addition, the density of states at the Fermi level of the FeMn to be calculated.

## II. EXPERIMENTAL DETAILS

All films were deposited on (100) oxidized silicon substrates by dc magnetron sputtering at 0.5 Pa, in an in-plane magnetic field $\mu_0 H \sim 40$ mT. The sputtering system was cooled with liquid nitrogen and had a base pressure better than $3\times10^{-9}$ mbar. The system was fitted with a load lock, which minimizes run to run variation by keeping the targets under constant vacuum. Deposition rates were of the order of 0.08 nm/s for the Cu, Co, and FeMn targets, and 0.03 nm/s for Nb. Film thicknesses were controlled by varying the exposure time under the magnetron targets. For all samples containing FeMn, a 5 nm underlayer of Cu was grown, in order to achieve the required fcc AF $\gamma$-FeMn phase.[18]

For the trilayer devices, a Nb/Cu/FeMn/Nb sandwich was grown *in situ*; FeMn thickness, $d_{FeMn}$ was in the range 2–6 nm, both Nb thicknesses were 150 nm. The films were patterned to micron scale wires with broad beam Ar ion milling (1 mA $cm^{-2}$, 500 V), and then processed with a Ga focused ion beam to achieve vertical transport with a device area in the range 0.25–1.2 $\mu m^2$. The fabrication process is de-

 

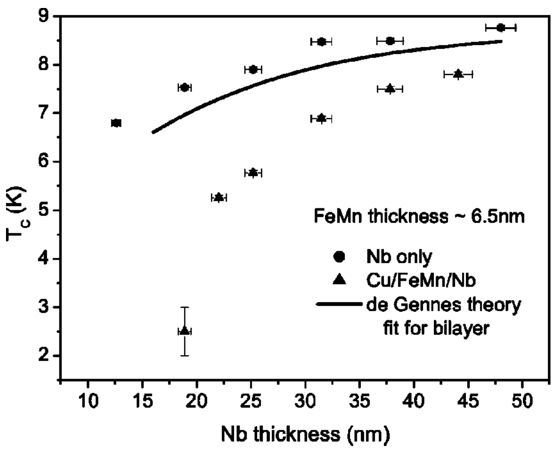


FIG. 1. Variation of $T_C$ vs Nb thickness for a constant FeMn thickness of 6.5 nm, (triangles), compared to plain Nb films (circles). Fit to triangles is de Gennes theory (see Sec. IV).

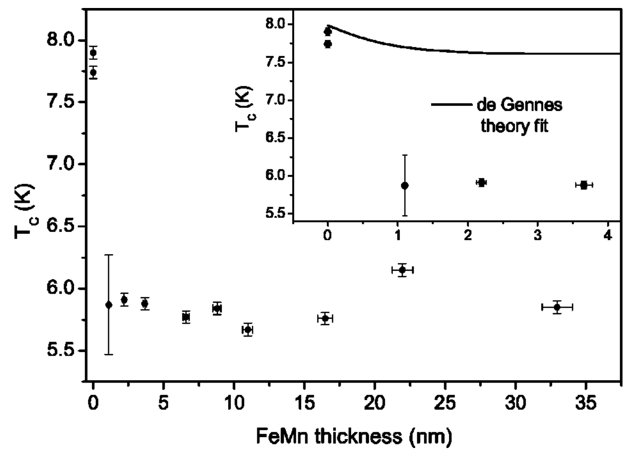


FIG. 2. Variation of $T_C$ vs FeMn thickness for a constant Nb thickness of 25 nm. Inset: detail for thinner films with de Gennes theory fit (see Sec. IV).

scribed in detail elsewhere.[19] For the bilayer measurements Cu/FeMn/Nb films were grown.

All transport measurements were made in a liquid He dip probe. The critical current ($I_C$) and normal state resistance ($R_N$) were measured with room temperature electronics. For devices with a $I_C R_N > 1\ \mu$V a current-voltage ($I$-$V$) characteristic was directly measured. For samples with $I_C R_N < 1\ \mu$V a differential resistance measurement was made with a lock-in amplifier, and the $I_C$ was found as a peak in the $dV/dI$ measurement. For the $T_C$ measurements a four-point configuration was used on unpatterned $5\times 10$ mm films. The rate of cooling was $<10^{-2}$ K/s near $T_C$.

## III. RESULTS

In this section the results of $T_C$ measurements on AF/$S$ bilayers are presented, followed by the measurements of $S$/AF/$S$ Josephson junctions.

### A. Measurements of $T_C$ in bilayers

Following Hübener *et al.*[4] we have measured the film $T_C$ independently varying the $S$ and AF thicknesses, as shown in Figs. 1 and 2, respectively. The $R(T)$ curves, showed a transition width of the order of 0.1 K, and the $T_C$ is defined as the midpoint of the transition. An absolute error of 0.05 K was found by measuring the $T_C$ of a thick Nb film, and repeated $T_C$ measurements show a relative error of $\sim 0.05$ K. For thicknesses of FeMn<1nm a broadened transition ($\sim 0.2$ K), is observed—presumably associated with large percentage variation of the film thickness over the substrate, and no consistent data was obtained in this thickness regime.

For a constant $d_{\mathrm{FeMn}} = 6.5$ nm, with varying Nb thickness, a suppression of $T_C$ was observed relative to the plain Nb film . In Fig. 1 the final point with $T_C < 4.2$ K was measured in a closed cycle He-3 cryostat, with a different calibration and thermal environment, hence the relative error in $T_C$ is larger.

For a constant Nb thickness of 25 nm the $T_C$ of the film drops dramatically as soon as the thinnest layer of FeMn is grown underneath (the two points at $d_{\mathrm{AF}} = 0$ in Fig. 2 are for Nb only and a Nb/Cu bilayer, respectively). This implies a short coherence length $\xi_{\mathrm{AF}}$ in the FeMn, which we will show correlates with the results from the Josephson junctions.

As a comparison, measurements on plain Nb films of decreasing thickness were also made, since in this thickness regime the Nb only film $T_C$ is also decreasing (circles in Fig. 1). The reduction can be attributed to a combination of grain size and resistivity effects, as well as the proximity effect.[20] The correlation between $T_C$ and resistance ratio $R(295\ \mathrm{K})/R(10\ \mathrm{K})$ (RRR) shown in Fig. 3 is associated with the grain size effect, and is consistent with previous studies.[21]

### B. Josephson junctions

The Josephson junctions showed resistively shunted junction (RSJ), $I$-$V$ characteristics, with $I_C$ in the range 10 $\mu$A to 1.2 mA, and $R_N \leqslant 2$ m$\Omega$. The reentrant $I_C(H)$ in Fig. 4

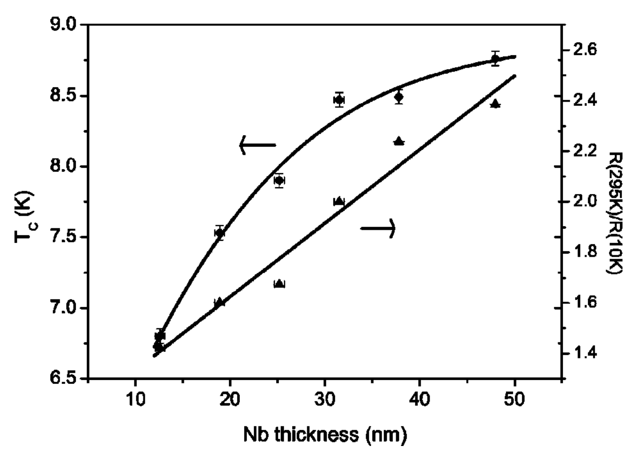


FIG. 3. $T_C$ and RRR variation vs thickness for Nb only films. Lines are the best fit cubic and linear curves for $T_C$ and RRR, respectively.

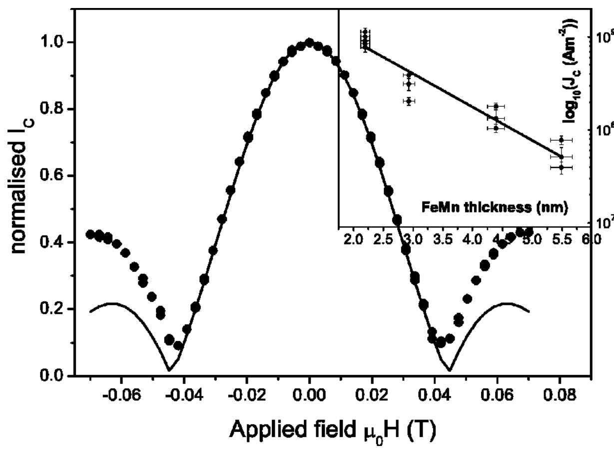


FIG. 4. Critical current modulation with an applied magnetic field, normalized to the zero field $I_C$. Line is a best-fit Fraunhofer pattern. Inset: Critical current density vs FeMn thickness for junctions at 4.2 K. Line is a best fit exponential $\exp(-2d_{\mathrm{AF}}/\xi_{\mathrm{AF}})$ with $\xi_{\mathrm{AF}}=2.4$ nm.

shows the presence of a Josephson current through the FeMn, although we do not obtain an ideal Fraunhofer pattern. In this case the modulation is normalized to zero field critical current $I_C=500$ $\mu$A. The junction dimension perpendicular to the direction of the applied field was $\sim$600 nm and the total barrier thickness (Cu and FeMn) was 7 nm. Correcting for the finite thickness of the Nb electrodes[22] (each is 150 nm thick) we obtain from the Fraunhofer fit a magnetic penetration depth of 40 nm. A voltage criterion is used to extract the $I_C$, hence the nonzero $I_C$ is an artifact of this process: the $I_C$ is suppressed to zero to within the 1 $\mu$V noise level of the measurement. We can estimate the Josephson penetration depth using $\lambda_J=(\hbar/2e\mu_0 J_C d)^{1/2}$. For the thinnest case with $d_{\mathrm{AF}}\sim 3$ nm and $J_C\sim 1\times 10^9$ A m$^{-2}$ we find $\lambda_J\sim 2$ $\mu$m, whereas the largest junction dimension is 1.2 $\mu$m, so we are close to long junction behavior only for the largest junction with the thinnest barriers.

The inset of Fig. 4 shows the variation of critical current density $J_C$ with $d_{\mathrm{FeMn}}$. Assuming a dirty $S/N/S$ junction $J_C\propto\exp(-k_{\mathrm{AF}}d_{\mathrm{AF}})$.[23] Using $k_{\mathrm{AF}}=2/\xi_{\mathrm{AF}}$ (see Sec. IV) and fitting this to the inset of Fig. 4, we find the characteristic decay length $\xi_{\mathrm{AF}}=2.4$ nm. The errors in $J_C(d)$ consist of measurement error of the submicron junction area, as well as scatter due to variation of $d_{\mathrm{AF}}$ over the area of the chip (this is also the case for the scatter in the $I_C R_N$ data of junctions with nominally the same thickness of FeMn). There may also be additional variation due to domain structures in the AF, and spin compensation at the interfaces which are spatially inhomogeneous. All devices for a given film thickness are patterned on the same 10 mm$\times$5 mm chip, hence interface transparency and contamination should be comparable for a given $d_{\mathrm{AF}}$.

## IV. DISCUSSION

$\gamma$-$Fe_{50}Mn_{50}$ (FeMn) is an example of a fcc disordered AF, and is one of the most studied materials used to exchange bias ferromagnetic films.[24] Although its magnetic/exchange bias properties have been intensively studied, the crystal structure is complex and difficult to probe, hence the precise nature of the magnetic structure of this material is still under debate.[25,26] The electronic properties are less well studied, and the authors are not aware of any experimental studies of properties such as the Fermi velocity, electronic heat capacity, or mean free path of FeMn thin films. In this section we use the measurements above to calculate some of the properties of the FeMn, and use them to fit the bilayer $T_C$ measurements.

If we consider FeMn as a band antiferromagnet the coherence length in the AF is given by (in the dirty limit)

$$\xi_{\mathrm{AF}}=\left[\frac{2\hbar D}{H_{\mathrm{ex}}}\right]^{1/2} \tag{1}$$

where $D=\frac{1}{3}v_{\mathrm{Fermi}}\ell$ is the diffusion constant and $H_{\mathrm{ex}}\sim k_B T_N$ the exchange coupling between the AF spins, similar to the exchange field in the ferromagnetic case. The additional factor of 2 compared to the F case $[\xi_F=(4\hbar D/H_{\mathrm{ex}})^{1/2}]$ arises since the AF wave vector has the form $k_{\mathrm{AF}}=2/\xi_{\mathrm{AF}}$ rather than the complex form $k_F=2(1+i)/\xi_F$ which gives rise to the oscillating order parameter in the $F$ case.[7] Hence, $\xi_{\mathrm{AF}}$ scales with the bulk $T_N$, which in the case studied here is in the range 450–490 K.[24] In the case of FeMn, however, because it is a highly disordered alloy system, we expect a very short mean free path $\ell$, of the order of 1 nm or less.[27] Hence, a reasonable value of $\xi_{\mathrm{AF}}$ using Eq. (1) with a Fermi velocity $v_{\mathrm{Fermi}}=2\times 10^6$ m s$^{-1}$ (both Fe and Mn have $v_{\mathrm{Fermi}}\sim 2\times 10^6$ m s$^{-1}$) is of the order of 4–5 nm. This is in agreement with the value from the trilayer junctions, and much shorter than the corresponding coherence length in a normal metal. Further information can be gained from this measurement of the coherence length. From Eq. (1) using $T_N=450$ K and $\xi_{\mathrm{AF}}=2.4$ nm, the diffusion constant $D$ is found to be $1.7\times 10^{-4}$ m$^2$ s$^{-1}$.

Given the value of the diffusion constant $D_{\mathrm{AF}}$ it is possible to calculate the density of states at the Fermi level using the Einstein relation $\sigma=2e^2\mathcal{N}(\epsilon_F)D$.[28] For this the value of $\sigma_{\mathrm{FeMn}}$ is required. This was found using a series of Cu(5 nm)/FeMn/Nb(6 nm) films grown for differing FeMn thicknesses (the Nb serves as a cap to prevent oxidation of the FeMn). Assuming a simple parallel resistor model, plotting the ratio of total thickness and resistivity against FeMn thickness should give a straight line with gradient equal to the conductivity of the FeMn. $\sigma_{\mathrm{FeMn}}$ is found to be $8.4\times 10^5(\Omega\ \mathrm{m})^{-1}$, from the linear fit (Fig. 5). Hence using $\sigma=2e^2\mathcal{N}(\epsilon_F)D$, with the values of $D$ and $\sigma_{\mathrm{FeMn}}$ above, the density of states at the Fermi level $\mathcal{N}(\epsilon_F)$ in FeMn is found to be $2.7\times 10^{25}$ states J$^{-1}$ m$^{-3}$. For parallel resistors, the intercept of Fig. 5 is given by $\sigma_{\mathrm{Nb}}d_{\mathrm{Nb}}+\sigma_{\mathrm{Cu}}d_{\mathrm{Cu}}$. Using the value of $\sigma_{\mathrm{Nb}}$ (see below) this intercept is predicted to be of the order of 0.16 $\Omega$. The smaller observed value is associated with interface resistance, which would be significant for $d_{\mathrm{Nb}}=6$ nm, which reduces the effective value of $\sigma_{\mathrm{Nb}}$. This is also consistent with a higher value of $\sigma_{\mathrm{FeMn}}$ obtained from the junction $R_N$ values: which would also contain a component due to the interface resistance.

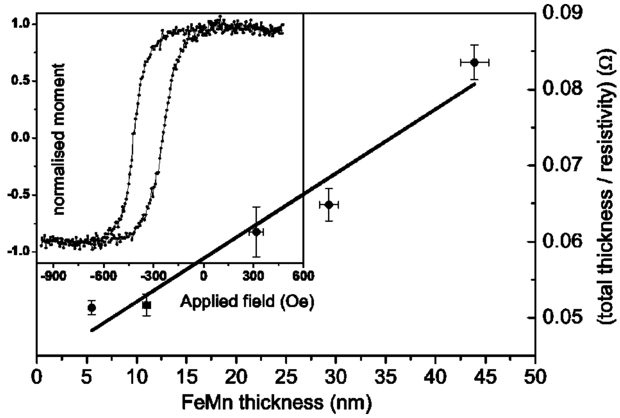


FIG. 5. Linear fit to find $\sigma_{\mathrm{FeMn}}$ using different thicknesses of FeMn in a Cu/FeMn/Nb trilayer, at 295 K. Inset: Hysteresis loop of a Nb/Cu/FeMn/Co/Nb trilayer after annealing at 0.2 T from 200 °C for 30 min.

We can now fit the bilayer $T_C$ measurements. We do not follow Ref. 4 which analyzed the data in terms of the Werthamer theory.[29] This considers the case that the metals are identical in the normal state, i.e., the Fermi velocities, residual resistivity, and Debye temperatures are the same, and uses a single effective coherence length. However, in this case the Nb and FeMn films are significantly different, and we should consider the coherence lengths of the superconductor and normal metal separately. Hence we use de Gennes theory in the one frequency approximation.[23] For the case that the normal metal film is not superconducting at any temperature, i.e., has $T_C=0$ K, we have

$$\frac{1}{\sqrt{2}\xi_S}\sqrt{\left(\frac{T_{CS}}{T_C}-1\right)}\tan\left[\frac{d_S}{\sqrt{2}\xi_S}\sqrt{\left(\frac{T_{CS}}{T_C}-1\right)}\right]$$
$$=\frac{2}{\xi_{\mathrm{AF}}}\frac{D_{\mathrm{AF}}\mathcal{N}_{\mathrm{AF}}(\epsilon_F)}{D_S\mathcal{N}_S(\epsilon_F)}\tanh\left[\frac{2d_{\mathrm{AF}}}{\xi_{\mathrm{AF}}}\right], \qquad (2)$$

where the largest root of this equation gives $T_C$, the transition temperature of the bilayer. Here $\mathcal{N}_{S,\mathrm{AF}}(\epsilon_F)$ are the density of states at the Fermi level of the $S$ and AF, respectively, and $T_{CS}$ the transition temperature of the plain $S$ layer. All of the required parameters for Eq. (2) are known, or can be obtained by experiment, as we now show.

From the trilayer junctions results above we use $\xi_{\mathrm{AF}}=2.4$ nm. The thicknesses $d_S$ and $d_{\mathrm{AF}}$ are known for a given film. To find $\xi_S$ in the dirty limit we use $\xi_S=0.85(\xi_0\ell)^{1/2}$, with $\xi_0\approx\hbar v_{\mathrm{Fermi}}/k_BT_0$ and substitute using the free electron form $D=\frac{1}{3}v_{\mathrm{Fermi}}\ell=\sigma k_B^2\pi^2/3e^2\gamma$.[4,30] We obtain

$$\xi_S=\left[\frac{\pi\hbar k_B\sigma}{6e^2\gamma T_0}\right]^{1/2}. \qquad (3)$$

Here the electronic specific heat capacity $\gamma=720\ \mathrm{J\,m^{-3}\,K^{-2}}$,[31] and $T_0=9.25$ K, the bulk $T_C$ of Nb. From a van der Pauw measurement at 295 K we find a value of $\sigma_{\mathrm{Nb}}=2.7\times10^7\ (\Omega\,\mathrm{m})^{-1}$ for our films. We use a linear fit to follow the variation of RRR value with $d_{\mathrm{Nb}}$, (Fig. 3). Hence for a given thickness of Nb we calculate $\sigma_{\mathrm{Nb}}(10\ \mathrm{K})$, using the RRR linear fit, and then find $\xi_S$ using Eq. (3). $\xi_S$ is found to be of the order of 6 nm.

The plain Nb transition temperature $T_{CS}$ is similarly followed using an empirical cubic fit to the $T_C$, as in Fig. 3. Finally from $\sigma=2e^2\mathcal{N}(\epsilon_F)D$ the ratio $D_{\mathrm{AF}}\mathcal{N}_{\mathrm{AF}}(\epsilon_F)/D_S\mathcal{N}_S(\epsilon_F)$ is identical to $\sigma_{\mathrm{FeMn}}/\sigma_{\mathrm{Nb}}=0.031$, using the above values. Hence the only remaining parameter in Eq. (2) is $T_C$, for which we solve numerically.

For varying Nb thickness, this fit with no adjustable parameters is shown as a solid line in Fig. 1, which is clearly not a good qualitative fit to the data. For the case of varying FeMn thickness, as can be seen from Fig. 2, the suppression of $T_C$ is saturated for thicknesses $>1$ nm: which would be expected for a coherence length of that order. The inset of Fig. 2 shows that the theoretical fit, which saturates for $d_{\mathrm{AF}}\geqslant2.5$ nm, although the saturation value of $T_C$ is much higher than found experimentally. With $d_{\mathrm{FeMn}}>10$ nm there does appear to be some additional variation of $T_C$, which is not expected from Eq. (2). However this most likely due to a different phase of FeMn being produced in films thicker than 20 nm.[18] More investigation of this behavior is required.

A Nb(150 nm)/Cu(5 nm)/FeMn/Co/Nb(150 nm) structure was also grown as a reference to check the AF nature of the FeMn, with $d_{\mathrm{FeMn}}\sim4.5$ nm, and $d_{\mathrm{Co}}\sim2$ nm. $M(H)$ hysteresis loop measurements were made with a vibrating sample magnetometer, and showed that there was some exchange bias associated with the applied field during deposition. The relatively weak nature of this ($H_{\mathrm{bias}}\sim150$ Oe) implies that there are many misaligned domains in the Co being pinned by the AF. The film was annealed in a field of 0.2 T at 200 °C for 30 min, and field cooled. After annealing the exchange bias was measured as $H_{\mathrm{bias}}\sim335$ Oe (inset of Fig. 5). This shows that the FeMn is an AF in this thickness regime, as expected. Although in this regime the magnitude of the exchange bias is changing with $d_{\mathrm{FeMn}}$,[32] this does not imply variation of the exchange coupling energy between the spins at 4.2 K, hence we can assume a constant value of $\xi_{\mathrm{AF}}$.

Many models of exchange bias in magnetic films use compensation of spins at the interface as a crucial parameter. Indeed the true structure of the present device might be $S/N/F/\mathrm{AF}/F/S$: where the $F$ layers are uncompensated AF spins. A full theoretical description of these bilayers and junctions may enable additional information concerning the nature of thin films of $\gamma$–FeMn to be gained, as well as provide a qualitative fit to the data in the present work.

## V. CONCLUSIONS

We have been able to obtain the diffusion constant $D$, and density of states of $\gamma$-FeMn. We have also fabricated AF Josephson junctions with a coherence length $\xi_{\mathrm{AF}}\sim2.4$ nm. This value of $\xi_{\mathrm{AF}}$ was used to model AF/$S$ bilayer $T_C$ measurements, and with no free parameters, but gave unsatisfactory results. It is clear that a more relevant theory is required to fit the data. Although this work implies a similar strong suppression of superconductivity in AF FeMn as in the ferromagnetic case, the thicknesses used in the present work are similar to those used to fabricate spin valves. Hence the fabrication of a Josephson spin valve using FeMn as a pinning layer, measured below 4.2 K may possess a $J_C$ which is not too small to be beyond experimental reach, although a AF with lower $T_N$, and weaker F layers would significantly increase the $J_C$ of the junctions.


## ACKNOWLEDGMENTS

We would like to thank Manna Ali (University of Leeds) for annealing the exchange biased film. This work was supported by the Engineering and Physical Sciences Research Council, UK.



[1] J.J. Hauser, H.C. Theuerer, and N.R. Werthamer, Phys. Rev. **142**, 118 (1966).
[2] Y. Cheng and M.B. Stearns, J. Appl. Phys. **67**, 5038 (1990).
[3] C. Attanasio, C. Coccorese, L.V. Mercaldo, M. Salvato, L. Maritato, S.L. Prischepa, C. Giannini, L. Tapfer, L. Ortega, and F. Comin, Physica C **312**, 112 (1999).
[4] M. Hübener, D. Tikhonov, I.A. Garifullin, K. Westerholt, and H. Zabel, J. Phys.: Condens. Matter **14**, 8687 (2002).
[5] V.V. Ryazanov, V.A. Oboznov, A.Y. Rusanov, A.V. Veretennikov, A.A. Golubov, and J. Aarts, Phys. Rev. Lett. **86**, 2427 (2001).
[6] T. Kontos, M. Aprili, J. Lesueur, and X. Grison, Phys. Rev. Lett. **86**, 304 (2001).
[7] V.N. Krivoruchko, Zh. Éksp. Teor. Fiz **109**, 649 (1996) [JETP **82**, 347 (1996)].
[8] Y.A. Izyumov, Y.N. Proshin, and M.G. Khusainov, Phys. Usp. **45**, 109 (2002).
[9] F.S. Bergeret, A.F. Volkov, and K.B. Efetov, Phys. Rev. Lett. **86**, 3140 (2001).
[10] A.A. Golubov, M.Y. Kupriyanov, and Y.V. Fominov, JETP Lett. **75**, 190 (2002).
[11] V.N. Krivoruchko and E. Koshina, Phys. Rev. B **64**, 172511 (2001).
[12] N.M. Chtchelkatchev, W. Belzig, and C. Bruder, JETP Lett. **75**, 646 (2002).
[13] X. Waintal and P.W. Brouwer, Phys. Rev. B **65**, 054407 (2002).
[14] J.Y. Gu, C.-Y. You, J.S. Jiang, J. Pearson, Y.B. Bazaliy, and S.D. Bader, Phys. Rev. Lett. **89**, 267001 (2002).
[15] H.C. Yang and D.K. Finnemore, Phys. Rev. B **30**, 1260 (1984).
[16] J. Niemeyer and G. von Minnigerode, Z. Phys. B: Condens. Matter **36**, 57 (1979).
[17] J.L. Paterson, J. Low Temp. Phys. **35**, 371 (1979).
[18] C. Tsang, N. Heiman, and K. Lee, J. Appl. Phys. **52**, 2471 (1981).
[19] C. Bell, G. Burnell, D.-J. Kang, R.H. Hadfield, M. Kappers, and M.G. Blamire, Nanotechnology **14**, 630 (2003).
[20] M.S.M. Minhaj, S. Meepagala, J.T. Chen, and L.E. Wenger, Phys. Rev. B **49**, 15 235 (1994).
[21] A. Andreone, A. Cassinese, M. Iavarone, R. Vaglio, I.I. Kulik, and V. Palmieri, Phys. Rev. B **52**, 4473 (1995).
[22] M. Weihnacht, Phys. Status Solidi **32**, K169 (1969).
[23] P.G. de Gennes, Rev. Mod. Phys. **36**, 225 (1964).
[24] J. Nogués and I.K. Schuller, J. Magn. Magn. Mater. **192**, 203 (1999).
[25] G.M. Stocks, W.A. Shelton, T.C. Schulthess, B. Újfalussy, W.H. Butler, and A. Canning, J. Appl. Phys. **91**, 7355 (2002).
[26] K. Nakamura, T. Ito, and A.J. Freeman, Phys. Rev. B **67**, 014405 (2003).
[27] P. L. Rossiter, *The Electrical Resistivity of Metals and Alloys* (Cambridge University Press, Cambridge, 1991).
[28] N. W. Ashcroft and N. D. Mermin, *Solid State Physics* (Holt-Saunders, Philadelphia, 1976).
[29] N.R. Werthamer, Phys. Rev. **132**, 2440 (1963).
[30] A.B. Pippard, Rep. Prog. Phys. **23**, 176 (1960).
[31] C. Poole, *Handbook of Superconductivity* (Academic Press, New York, 2000).
[32] R. Jungblut, R. Coehoorn, M.T. Johnson, J. aan de Stegge, and A. Reinders, J. Appl. Phys. **75**, 6659 (1994).